Spinodal decomposition of a three-component water-in-oil microemulsion system

F. Mallamace,[1] N. Micali,[2] S. Trusso,[2] and S. H. Chen[3]
[1]*Department of Physics, University of Messina, Vill. S. Agata, C.P. 55, 98166 Messina, Italy*
[2]*Institute of Spectroscopic Techniques, Consiglio Nazionale delle Ricerche, Vill. S. Agata, Salita Sperone 31, 98166 Messina, Italy*
[3]*Department of Nuclear Engineering, 24-209, Massachusetts Institute of Technology, Cambridge, Massachusetts 02139*
(Received 8 December 1994)

We have performed a series of spinodal decomposition measurements of a three-component microemulsion system made of a surfactant Aerosol OT, water, and decane. The measurements were made by a temperature jump from a one-phase droplet microemulsion to a two-phase droplet microemulsion along the critical isovolume fraction line (10%) using a time resolved light scattering intensity measurement technique. All three stages of the evolution were studied. Time evolution of intensities for the initial stage follows closely the linearized theory. On the other hand, time evolution of the characteristic wave vector, the maximum scattering intensity, and the intensity distributions in the intermediate and late stages are in good agreement with recent dynamic scaling theories.

PACS number(s): 82.70.Kj

I. INTRODUCTION

A large number of studies have been carried out about the dynamics of phase separation. Examples of well studied systems are binary mixtures of molecular fluids, binary alloys, and polymer blends. The dynamics of phase separation, in all these systems, following a thermal quench into the unstable coexistence region, proceeds either by nucleation growth or spinodal decomposition (SD) [1,2]. Immediately after the quench, small domains, with local concentration roughly corresponding to that of the two main phases, spontaneously form and grow with time and finally result in a complete phase separation. As the mixture evolves towards its equilibrium state, the strong nonlinearity of the decomposition process produces an interconnected morphology that coarsens with time. The time evolution of SD in a system near its critical point has especially attracted much attention because the dynamics of the ordering process can be described from the viewpoint of both the universality of critical phenomena and the dynamical scaling concept.

Recently, attention has been focused on the dynamics of phase separation in glasses, polymer melts, gels, and microemulsions, which are generally called "complex fluids." In such systems the dynamics, reflecting their complex interconnected structure, is characterized by slow relaxation processes [3]. This implies existence of competing phenomena that can interfere with the phase separation. However, complex systems, owing to their longer characteristic relaxation times as compared to those occurring in simple fluids, allow for the investigation of SD in a much wider range of phase space possible than for simple liquid mixtures.

The entire time behavior of SD can be characterized by three different stages, namely, the early, the intermediate, and the late stages [4]. The linearized theory [5], the scaling concept [6], and more recently molecular dynamics (MD) simulations [7–10] have given a great impetus to the study of the growth and the time evolution of composition fluctuations in such systems. Whereas the early and the intermediate stages of systems studied so far show a universal behavior well accounted for by theoretical models, the late stage behavior is strongly dependent on the specific system properties. In this stage, simple binary mixtures and complex fluids show different behaviors. In particular, in complex systems, well defined slowing-down [7] and pinning phenomena [9] in the structure factors can be observed due to strong interactions or to the presence of a persistence length.

Careful attention has recently been devoted to the study of SD in binary mixtures containing surfactant. In fact, depending on the amount of surfactant in the solution, such a system can show a behavior that ranges from that of a simple critical mixture to that of a complex system. One possible reason is that such a system, depending on the surfactant concentration, can adopt many different structural arrangements. Recent MD simulations [7,10] have given some new insights into the phase separation process in such a complex system that can be summarized in the following way: (i) The structure factor for systems containing surfactant is different from that for binary mixtures without surfactant. (ii) For complex systems there is different late stage decomposition behavior for the case of an irregular bicontinuous microstructure and for the case of formation of micellar domains. (iii) For moderate surfactant concentrations the low interfacial tension of the surfactant adsorbed interface behaves in such a way that, in the late stage, the coarsening of the domain structures is considerably slowed down. (iv) The domain formation is accelerated by thermal fluctuations. (v) The phase separation in systems with different surfactant concentrations follows a crossover scaling function.

On these bases we have conducted extensive experimental studies of the SD in binary and ternary mixtures, with the presence of surfactant, as a function of the surfactant concentration by means of time resolved light scattering intensity measurements. Here in this paper we report the preliminary results of dynamics of phase separation in a three-component microemulsion system made

of an ionic surfactant aerosal OT (AOT) (sodium di-2 ethylhexlylsulfosuccinate), water, and decane at the critical composition.

Many careful experiments [11] have given a definite conclusion that the microemulsion, for a constant [water]/[AOT] molar ratio (indicated as w), can be effectively considered as a pseudobinary system. More precisely, it has been shown that the system at constant pressure and constant w can be treated thermodynamically as a two-component system consisting of surfactant-coated water droplets of a specific average radius, depending on the w value, dispersed in oil. Thus one can apply the equations of the mode-coupling theory developed for the critical dynamics in binary fluid mixtures to study the equilibrium dynamic critical phenomena of this type of microemulsion [12].

II. EXPERIMENT

The experimental setup used has already been fully described elsewhere [13]. The most important feature is that it works in Fourier transform scattering geometry in order to increase the signal-to-noise ratio. To minimize multiple scattering effects, we used a quartz cell with 1 mm thickness. The sample optical cell was thermostated with a temperature regulation of better than ± 1 mK. Each scan over the 1024 channels of the linear position sensitive detector covering the range of wave number $Q = 0.1 - 0.94\ \mu\text{m}^{-1}$ [$Q = (4\pi n/\lambda)\sin(\theta/2)$] is performed every 30 msec. Here n, λ, and θ are the refractive index of the sample, the wavelength of the incident beam (6328 Å), and the scattering angle, respectively.

The AOT-water-decane microemulsion system shows, in a given w range, a liquid-liquid critical point characterized by a diverging correlation length ξ and a critical slowing down of the order parameter fluctuation [11]. The phase separation occurs upon raising the temperature. Above T_c the microemulsion separates into two microemulsion phases with similar microemulsion droplets, but having different volume fractions of surfactant-coated water droplets (η = volume fraction of water plus surfactant). Small-angle neutron scattering (SANS) experiments performed in the critical region have shown that the order parameter is the volume fraction ζ. By fixing $w = 40.8$, the critical volume fraction is $\eta_c = 0.098$ and the critical temperature $T_c = 39.860\,^{\circ}\text{C}$ [11]. Figure 1 shows the normalized form of the T-η phase diagram of the AOT-water-decane microemulsion system at $w = 40.8$ [14]. It should be noted that there is an additional feature in this phase diagram which is the percolation line (determined by electrical conduction measurements). It starts from the vicinity of the critical point, cutting across the whole phase diagram, having progressively decreasing percolation temperatures as the volume fraction increases. The complete features of the phase diagram, including the coexisting line, spinodal line, and percolation line, can be accounted for in terms of Baxter's sticky sphere model [15].

The samples have been prepared using a well established procedure [11]. The phase separation was initiated by a thermal quenching with a quick (lower than 0.1 sec)

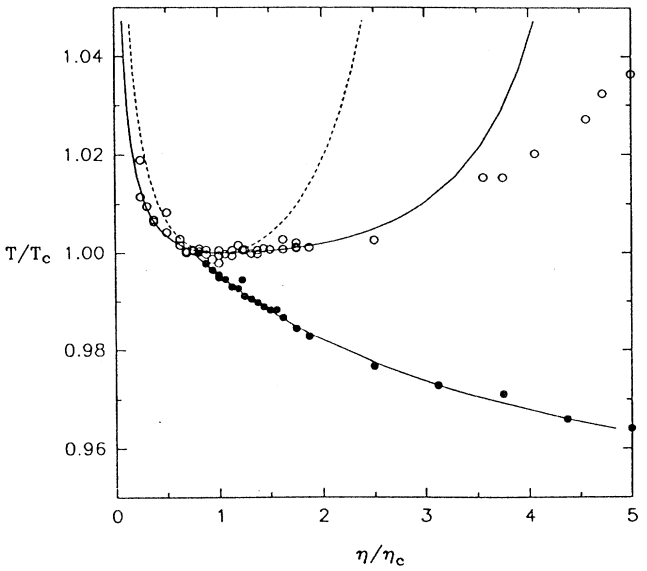

FIG. 1. Normalized phase diagram of the AOT-water-decame droplet microemulsion system, at $w = 40.8$ and ambient pressure, on the temperature-volume fraction (of the droplets) plane. The critical temperature $T_c = 40.8\,^{\circ}\text{C}$ and the critical volume fraction $\eta_c = 0.098$. The open circles indicate the phase boundary and solid circles the percolation locus obtained from experiments [14]. Solid and dotted lines indicate, respectively, the theoretical coexistence and percolation line and the spinodal curve obtained by using Baxter's sticky sphere model [15].

increase of the temperature from a temperature 0.02 K below T_c to a temperature T_f above but close to T_c ($T_f - T_c \approx 0.05$ K). The scattering intensities for different quench depths $\Delta T = T_f - T_c$ ranging from 0.02 K up to 0.5 K above T_c were measured. Corrections for the background and attenuation of light through the sample were carried out.

III. RESULTS AND DISCUSSION

SD appears as a ring of scattered light just after the quench. In the early stage the radius of the ring remains constant but the intensity of the ring increases with time. In this stage the Cahn and Hilliard [5] theory, based on linearization of a generalized diffusion equation, describes well the time dependent behavior of the growth of the composition fluctuation and thus also the intensity increase. After this stage, the wave number of the dominant fluctuating mode decreases with time and the decomposition enters the intermediate stage. Whereas in the early stage the mechanism of the decomposition is explained in terms of the negative curvature of the free energy, which makes the diffusion constant negative (particles move from rare to dense regions), in the intermediate stage the driving force for the droplet growth is the surface tension. In this stage the scaling concept is appropriate for the description of the growth rate of coalescing domains [6]. In particular, it has been shown that the scattering intensity $I(Q,t)$ scales as $F(Q/Q_1) = Q_1^3 I(Q,t)$, where Q_1 is the first moment of

the scattering intensity. As a typical example, the time evolution of scattering intensities for the quench depth $\Delta T=0.05$ K is shown in Fig. 2. Figure 2(a) depicts intensities corresponding to the early to intermediate stages. As one can see, initially, the scattered intensity increases with time but with almost no change of the wave number at the maximum intensity until one reaches the intermediate stage. In the figure, the thick line connects all the peak positions, from which one can discern the transition point of the early to intermediate stages. Figure 2(b) gives the scattering intensities in the late stage.

In order to test the validity of the linearized theory for the early stage from the measured scattering intensities we adopt the $\frac{1}{3}$ power plot used by Sato and Han [17] based on modification of the linearized theory of Cahn and Hilliard. In this theory, the scattering intensity $I(Q,t)$ including the thermal noise effect is written as

$$I(Q,t)=I_X(Q)+[I_0-I_X(Q)]\exp[2R(Q)t] , \quad (1)$$

where $I_X(Q)$ is the virtual intensity arising from the thermal noise, I_0 the intensity at time $t=0$. The growth rate $R(Q)$ is related to the mobility M, the composition susceptibility χ, the interdiffusion coefficient D^*, and a constant κ (related to the interfacial free energy) by

$$R=-MQ^2(\chi^{-1}+2\kappa Q^2)=D^*Q^2(1-Q^2/2Q_m^2) , \quad (2)$$

with $Q_m=\frac{1}{2}(D^*/M\kappa)^{1/2}=Q_m(0)$. Q_m is the wave number where the growth rate has the maximum value and should coincide with the wave number corresponding to the peak intensity $Q_m(t)$ at $t=0$. The $\frac{1}{3}$-power plot of Sato and Han written down in the following:

$$\{t/[I(Q,t)-I(Q,0)]\}^{1/3}=\{2R(Q)[I(Q,0)-I_X(Q)]\}^{-1/3}\{1-\tfrac{1}{3}R(Q)t+\tfrac{1}{81}[R(Q)t]^3+\cdots\} \quad (3)$$

can be used to obtain the growth rate $R(Q)$. As the second-order term in t is absent in Eq. (3), this equation can be well approximated by a linear equation, so that the growth rate can be obtained by a linear fitting. Thus the $R(Q)$ values obtained from Eq. (3) at various Q values are plotted as R/Q^2 vs Q^2. The intercept of this line with the abscissa gives $2Q_m^2$ whereas that with the ordinate gives D^*. In Fig. 3 we give the result of such a plot. One can observe from the R/Q^2 vs Q^2 plot for $\Delta T=0.05$ K a linear behavior as stated. From the fact that values of Q_m obtained with this procedure are in complete agreement with initial peak positions of the scattering intensities against Q plots, it is confirmed that the early stage of SD exists and the linearized theory is valid.

A scaling concept for the kinetics of phase separation has been proposed to characterize the behavior of $Q_m(t)$ and $I_m(t)$ with time. $Q_m(t)$ here represents the wave number corresponding to the maximum scattered intensity $I_m(t)$. In this theory $Q_m(t)$ and $I_m(t)$ are expressed by simple power-law relations as $Q_m(t)\sim t^{-\alpha}$, and $I_m(t)\sim t^{-\beta}$. In particular, the scaling idea was extended to the later stage where a self-similar structure develops in the system and a single length scale describing such a structure is assumed to exist. The relevant length scale ξ^* and the wave vector Q_c are determined by the early stage behavior as $Q_c=Q_m(0)$ and $\xi^*=Q_c^{-1}$. The characteristic time t_c is related to ξ^* and the interdiffusion coefficient D^* by $t_c=\{D^*[Q_m(0)]^2\}^{-1}$. ξ^* and D^* are expected to behave similarly with the correlation length and the diffusion coefficient in the stable one-phase region. By means of t_c and Q_c, the time evolution of the phase separation process is expressed by a dimensionless scaled relation as

$$Q_m(\tau)=Q_m(t)/Q_m(0)\sim\tau^{-\alpha} \text{ with } \tau=t/t_c . \quad (4)$$

In critical binary mixtures, when hydrodynamic effects are considered, the exponent α can change form 0 to 1 from the early to the late stages of SD [1,2,4]. In the intermediate stage where the Brownian coagulation occurs, $\alpha=\frac{1}{3}$. The deviation of a from zero defines the onset of the intermediate stage where $\beta>3\alpha$. In the late stage where the system dynamics is dominated by mass flow, a changes from $\frac{1}{3}$ to 1. In this stage $\beta=3\alpha$ and

$$[Q_m(\tau)]^3I_m(\tau)\sim\tau^0 . \quad (5)$$

From the scaling relation $F(Q/Q_1)=Q_1^3I(Q,t)$ we have $[Q_m(\tau)]^3I_m(\tau)\sim F(Q/Q_m(\tau))$. The scaled structure factor is usually defined as [6]

$$\overline{F(X)}=F(X)/\int F(X)X^2dX \text{ with } X=Q/Q_m(\tau) . \quad (6)$$

From the viewpoint of the scaling concept in the dynamics of SD, Furukawa proposed [6], for the region of self-similarity in the structure, the form

$$\overline{F(X)}=X^\delta/[\gamma^{/\delta}+X^{(\gamma+\delta)}] . \quad (7)$$

This form suggests that $\overline{F(X)}=X^\delta$ for $X\ll 1$, and $\overline{F(X)}=X^{-\gamma}$ for $X\gg 1$. In the late stage of the decomposition, the tail of the structure factor (large Q) follows Porod's law; it behaves in fact as Q^{-4}, indicating the formation of a sharp interface ($\gamma=4$). For conservative systems $\delta=4$ is predicted (thermal fluctuations are not effective, otherwise $\delta=2$) for three-dimensional space. Therefore an X^{-6} dependence is predicted for $X>1$. The scaling behavior of the structure factor suggests the existence of a single-length parameter describing the formation of the self-similar structure in the phase separating system. The scaling in the structure factor should also be related to the Q dependence of the dominant peak of the fluctuation modes. An additional feature of the scattering functions in the late stage is the presence of a shoulder in the larger scattering-angle region of the dominant

peak. This shoulder, theoretically predicted by taking into account long-range hydrodynamic interactions [16], has been observed in different systems [4].

Figure 4 summarizes the scaled time dependence of $Q_m(\tau)$, the scaled wave number at the maximum of the scattering intensity distribution, for two different thermal quenches, i.e., $\Delta T=0.05$ K and $\Delta T=0.03$ K. Each curve of $Q_m(\tau)$ as a function of the scaled time τ for different ΔT coincides with each other. As can be observed, the exponent α is time dependent reflecting cross-over among various coarsening mechanisms. This behavior was predicted by the theories of Kawasaki and Ohta [16] and Furukawa [6]. The crossover of α form 0 to $\frac{1}{3}$ occurs at $t \approx 1$ in complete agreement with other experimental results in simple critical mixtures and theoretical models [1,2,10,16]. In this time regime, the growth mechanism is dominated by hydrodynamic effects [16] and the $\frac{1}{3}$ power law is reminiscent of a diffusive mechanism. In the late stage, the establishment of interfaces and the existence of gravity can modify the growth

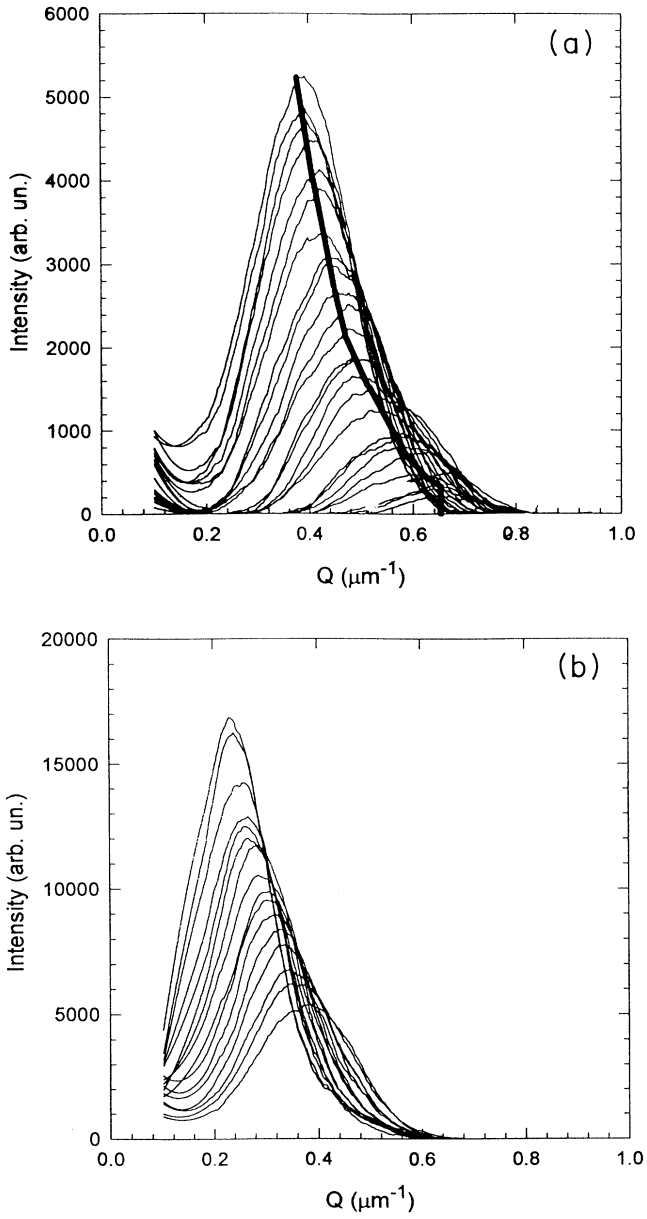

FIG. 2. Time evolution of the light scattering intensity distribution following a quench of depth $\Delta T=0.05$ K. (a) depicts intensities corresponding to the early and intermediate stages (the thick line connects all the peak positions) and (b) depicts those of the late stage.

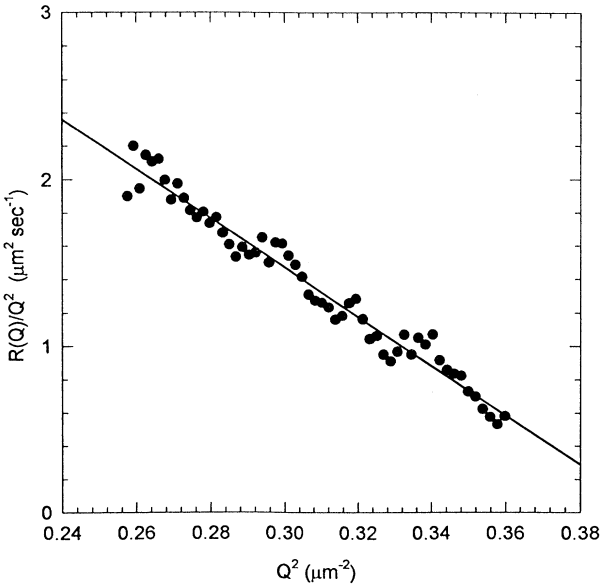

FIG. 3. The growth rate $R(Q)$ obtained from the $\frac{1}{3}$ power plot of Sato and Han [17] plotted as R/Q^2 vs Q^2. The intercept of the line with the abscissa gives $2(\xi^*)^{-2}$ and with that of the ordinates give D^*.

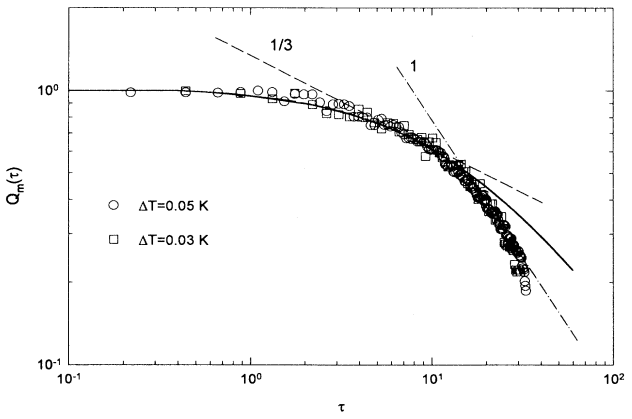

FIG. 4. Time evolution of the scaled wave number at the peak intensity after depths of quench $\Delta T=0.05$ K and $\Delta T=0.03$ K. The solid line is the result of a fit to an analytical function developed by Furukawa [6]. As can be seen, the early stage picture holds for the scaled time interval $0<\tau<2$, the intermediate stage for $2<\tau<18$, and the late stage for $\tau>18$.

behavior. For example, when the two phases are interconnected, capillary instabilities can appear [2,18] that give rise to a power law with $\alpha \approx 1$. The master curve shows no evidence of pinning or slowing down at large times as proposed by MD simulations [7,9] for a three-component system containing surfactant. On the contrary, we can observe for $\tau > 20$, $\alpha = 1$ growth law behavior characteristic of the late stage in fluid systems quenched into a regime where there are interconnected domains and the surface tension effects due to differences in concentrations between the separating phases leading to a crossover from $\frac{1}{3}$ to 1 power-law time dependence. In Fig. 4 we plot by a solid line the prediction of an analytical equation given by Furukawa [6] which describes the time-scaling behavior of $Q_m(\tau)$ in different stages of spinodal decomposition. This equation displays a well defined crossover regime and is applicable only to fluids in the critical region neglecting gravity effects. The curve is generated by setting the parameter $A = 0.1$ and obtaining the parameter $B = 0.054$ from a fitting procedure. The choice of $A = 0.1$ is made in order to reproduce the evolution behavior predicted for the intermediate stage by Kawasaki-Ohta theory [16]. It can be seen that we obtain a very good agreement between the theory and experiment for data in the range of early to intermediate stages. The value of B we obtained is of the same order of magnitude as those reported in the literature ($0.02 < B < 0.14$) [6,4]. For our data the Furukawa equation does not work for $\tau > 18$, where there is a crossover from the intermediate to the late stage. Compared with typical results of simple binary mixtures, our microemulsion system shows an onset of the late stage at a relatively low value of the reduced time. This can be explained by considering that at the relatively large quench depths ($\Delta T = 0.05$ and 0.03 K) we have, there are large differences in concentrations of the two phase-separated microemulsions and consequent large interfacial tensions between the two.

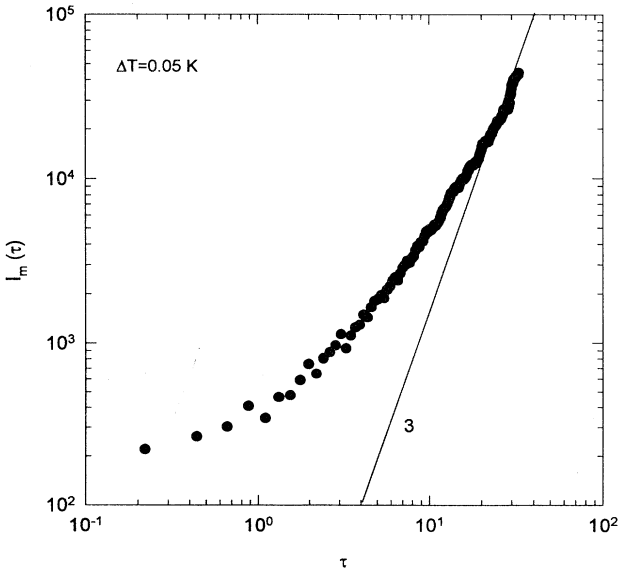

FIG. 5. The peak intensity $I_m(\tau)$ vs τ for the quench depth $\Delta T = 0.05$ K. As can be seen, in the late stage of the SD, the peak intensity approaches a τ^3 dependence ($\beta = 3\alpha$).

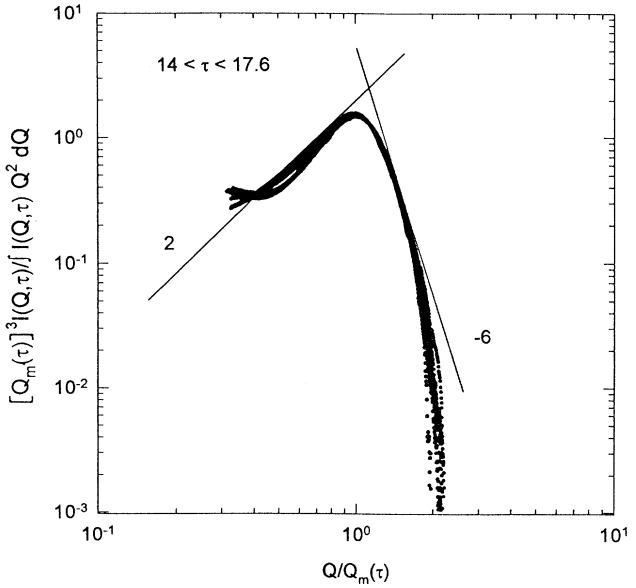

FIG. 6. The scaled intensity distributions (about 30 of them) measured in the scaled time interval $14 < \tau < 17.6$ (the intermediate stage). The scaled intensities show the universal behavior given by the theoretical models based on the scaling concept [1,6].

Figure 5 summarizes the scaled-time dependence of the spinodal ring intensity $I_m(t)$ for $\Delta T = 0.05$ K. As can be seen, a log-log plot of $I_m(\tau)$ vs τ attains the slope $\beta = 3$ in the time domain $\tau \geq 20$, whereas the intermediate stage is

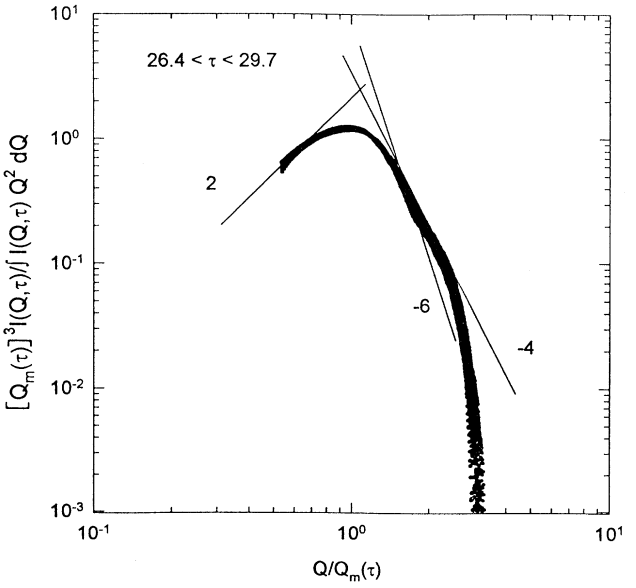

FIG. 7. The scaled intensity distributions (about 30 of them) measured in the scaled time interval $26.4 < \tau < 29.7$ (late stage). The scaled intensities in this case show also the predicted universal behavior. In particular, one can observe the presence of a shoulder indicating the onset of the Q^{-4} (Porod) behavior after the Q^{-6} region.

confined to $1<\tau<20$. This means that (in agreement with the theoretical suggestions) in the late stage $\beta=3$ and $\alpha=1$. The feature $\beta=3\alpha$ implies that a self-similar structure is formed which is characteristic of the ordering process in the late stage. On the other hand, in the intermediate stage one has $\beta>3\alpha$.

The scaled structure factors vs the scale variable $X=Q/Q_m(\tau)$ as defined by Eq. (6) are shown in Figs. 6 and 7 for $\Delta T=0.05$ K at different ranges of τ so as to cover the range from the intermediate to the late stages where the dynamical scaling holds. These two stages are considered separately. We do not consider here the Q behavior of the scaled structure factor in the early stage, because it has been well accounted for by the Sato and Han [17] analysis used for the evaluation of $Q_m(0)$ and D^*. In Fig. 6 all the scaled structure factors within the elapsed times in the range $14<\tau<17.6$ (intermediate stage of SD) are superposed. It can be observed that the wave vector scaling behavior agrees with Furukawa's predictions [6]. In particular, we have $F(X)=X^2$ for $X\ll 1$ ($\delta=2$) and $F(X)=X^{-6}$ for $X\gg 1$ ($\gamma=6$). The scaling behavior observed in the late stage is, however, different and shown in Fig. 7 for $26.4<\tau<29.7$. Whereas for small $X(Q<Q_m)$ we have again an X^2 dependence, for $Q>Q_m$ we observe a shoulder located at $Q=2.5Q_m$ and an onset of the Porod behavior (Q^{-4}) for $X>20$. The Q^{-6} scaling can only be observed in a range $1.5<Q/Q_m<2$. Thus the theoretical predictions based on scaling argument [6] hold also in this stage.

IV. CONCLUSION

In conclusion we observe that the kinetics of the phase separation process in a three-component water-in-oil microemulsion system, at the critical volume fraction, follows the same behavior exhibited by simple critical mixtures studied before [4]. The time evolution of the peak scattering intensity and the intensity distribution in the early stage are described satisfactorily by means of the linearized theory of SD [5]. On the other hand, the kinetics of the SD process, in both the intermediate and the late stages, are well accounted for by the use of the scaling concept. A comparison of the obtained data in the late stage with the main results of a recent MD simulation [7], carried out for binary mixtures containing surfactant, gives an indication that in the investigated system the separation occurs through the formation of irregular bicontinuouslike domains. In fact, aside from the fact that the hydrodynamic effects were not taken into account in the MD simulation, we noted that the behavior of the measured scaled-time evolution of the scaled wave number $Q_m(\tau)$, shown in Fig. 4, is similar to that obtained by the MD simulation for a binary mixture containing a very low amount of surfactant. In this case, the SD process is said to be dominated by the bicontinuous microstructure of the system (see Figs. 4, 8, and 10 of Ref. [7]). In this regard, we may stress that in the system investigated in our experiment the volume fraction of the surfactant is $\eta_S\approx 0.01$. For this microemulsion system at 10% volume fraction, as can be seen from the phase diagram in Fig. 1, the critical point is above the percolation point. Perhaps percolated droplet microemulsions, as studied extensively by one of us near the critical point by the Baxter model [15], have a similar structural effect on the phase separation kinetics as a bicontinuous one simulated in MD. MD results for systems with higher surfactant volume fractions or systems having a micellar structure are very different from that having a bicontinuous structure. In the MD, a marked slowing down of the time evolution of $Q_m(\tau)$ is quite evident for a micellar system.

ACKNOWLEDGMENT

Research work of S.H.C. is supported by the U.S. Department of Energy.

[1] For a recent review, see K. Binder, in *Material Science and Technology: Phase Transformation in Materials,* edited by P. Hansen (VCH, Weinham, 1990), Vol. 5, pp. 405–471.

[2] W. I. Goldburg, in *Scattering Techniques Applied to Supramolecular and Nonequilibrium Systems,* edited by S. H. Chen, B. Chu, and R. Nossal (Plenum, New York, 1981).

[3] *Dynamics and Patterns in Complex Fluids,* edited by A. Onuki and K. Kawasaki (Springer, Heidelberg, 1989); *Slow Dynamics in Condensed Matter,* edited by K. Kawsaki, M. Tokuyama, and T. Kawakatsu (AIP, New York, 1992).

[4] K. Kubota, N. Kuwahara, H. Eda, M. Sakazume, and K. Takiwari, J. Chem. Phys. **97**, 9291 (1992); Phys. Rev. A **45**, R3377 (1992).

[5] J. W. Cahn and J. E. Hilliard, J. Chem. Phys. **28**, 258 (1958).

[6] See, e.g., H. Furukawa, Adv. Phys. **34**, 703 (1985).

[7] T. Kawakatsu, K. Kawasaki, M. Furusaka, H. Okabayshi, and T. Kanaka, J. Chem. Phys. **99**, 8200 (1993).

[8] A. Shinokazi, and Y. Oono, Phys. Rev. E **48**, 2622 (1993).

[9] S. C. Glotzer, M. F. Gyure, F. Sciortino, A. Coniglio, and H. E. Stanley, Phys. Rev. E **49**, 247 (1994).

[10] M. Laradji, O. G. Mouritsen, S. Toxvaerd, and M. J. Zuckermann, Phys. Rev. E **50**, 1243 (1994).

[11] M. Kotlarchyk, S. H. Chen, J. S. Huang, and M. W. Kim, Phys. Rev. A **28**, 508 (1933); **29**, 2054 (1984); J. Rouch, A. Safouane, P. Tartaglia, and S. H. Chen, J. Chem. Phys. **90**, 3756 (1989).

[12] K. Kawasaki, Ann. Phys. (N.Y.) **61**, 1 (1970).

[13] S. H. Chen, D. Lombardo, F. Mallamace, N. Micali, S. Trusso, and C. Vasi, Prog. Colloid Polym. Sci. **93**, 311 (1993).

[14] C. Cametti, P. Codestefano, P. Tartaglia, J. Rouch, and S. H. Chen, Phys. Rev. Lett. **64**, 1461 (1990).

[15] C. Y. Ku, S. H. Chen, J. Rouch, and P. Tartaglia, Int. J. Thermophys. (to be published); S. H. Chen *et al.*, J. Phys. Condens. Matter **6**, 10 855 (1994).

[16] T. Ohta and H. Nozaki, in *Space-time Organization in Macromolecular Fluids,* edited by F. Tanaka, M. Doi, and T. Ohta (Springer, New York, 1989); T. Koga and K. Kawasaki, Phys. Rev. A **44**, 817 (1991).

[17] T. Sato and C. C. Han, J. Chem. Phys. **88**, 2057 (1988).

[18] E. D. Siggia, Phys. Rev. A **20**, 595 (1979).